

Dynamic Sampling for Deep Metric Learning

Chang-Hui Liang
Xiamen University
Xiamen, China

chliang@stu.xmu.edu.cn

Wan-Lei Zhao
Xiamen University
Xiamen, China

wlzhao@xmu.edu.cn

Run-Qing Chen
Xiamen University
Xiamen, China

chenrq1010026261@stu.xmu.edu.cn

Abstract

Deep metric learning maps visually similar images onto nearby locations and visually dissimilar images apart from each other in an embedding manifold. The learning process is mainly based on the supplied image negative and positive training pairs. In this paper, a dynamic sampling strategy is proposed to organize the training pairs in an easy-to-hard order to feed into the network. It allows the network to learn general boundaries between categories from the easy training pairs at its early stages and finalize the details of the model mainly relying on the hard training samples in the later. Compared to the existing training sample mining approaches, the hard samples are mined with little harm to the learned general model. This dynamic sampling strategy is formularized as two simple terms that are compatible with various loss functions. Consistent performance boost is observed when it is integrated with several popular loss functions on fashion search, fine-grained classification, and person re-identification tasks.

1. Introduction

Distance metric learning (usually referred to as metric learning), aims at constructing a task-specific distance measure based on given data. The learned distance metric is then used to support various tasks such as classification, clustering, and retrieval. Conventionally, the metric learning is designed to learn a matrix for the parametric *Mahalanobis* distance. Such that the similar contents are close to each other under the learned *Mahalanobis* distance, while the distance between the dissimilar contents is large.

Due to the great success of deep learning in many computer vision tasks in recent years, it has been gradually introduced to metric learning, which is widely known as deep metric learning. Instead of learning the distance metric directly, deep metric learning learns feature embedding from the raw data. For instance, given images x_a , x_b and x_c , x_a

and x_b are from the same category while x_c is distinct from them. The deep metric learning learns a non-linear mapping function $\mathcal{F}(\cdot)$ that embeds x_a , x_b and x_c to the new feature space. In this embedding space, $\mathcal{F}(x_a)$ and $\mathcal{F}(x_b)$ are close to each other, and $\mathcal{F}(x_c)$ is dissimilar to both of them under a predefined distance metric $m(\cdot, \cdot)$.

Owing to the seminal learning framework from [1], deep metric learning has been successfully adopted in various tasks such as online fashion search [8, 13, 4, 10], face recognition [1, 18], person re-identification [26], and fine-grained image search [19, 15, 24], etc. In general, the embedding space is learned on image pairs/triplets driven by loss functions. Namely, the training images are organized into positive pairs (images from the same category) and negative pairs (images from different categories). The loss function is designed to distill all the pair-based category information into a single loss value. The training process aims to build an embedding space by minimizing this loss. Such that the pairwise relations reconstructed in the embedding space coincide well with that of being supplied to the training. Since the number of pairwise relations is quadratic to the size of training image set, it is computationally expensive to enumerate all the pairwise relations of the training set. As a consequence, the definition of loss function along with the ushered-in pair-sampling strategy becomes critical. The general framework of deep metric learning is shown in Fig. 1.

In the literature, a series of loss functions have been proposed one after another. *Contrastive loss* [5] and *triplet loss* [7] are the two most popular loss functions. However, both of them fail to make full use of the pairwise relations in a mini-batch. In addition, it is widely observed that the large portion of image pairs are easy training samples. Hard training samples, which take up a small portion, are more decisive to the category boundaries. Due to the lack of strategy to mine on these hard training samples, deep metric learning based solely on *contrastive loss* and *triplet loss* converges slowly. To alleviate this issue, *N-Pair loss* [19], *lifted structure loss* [15], and *multiple similarity loss* [24] consider more pairwise relationships within one mini-batch.

¹This paper has been submitted to "Pattern Recognition Letters"

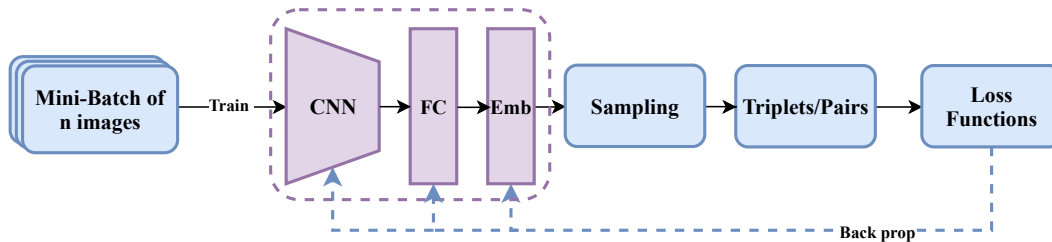


Figure 1. The general framework of deep metric learning. The training images are organized into mini-batches. Images are then forward to a pre-trained ConvNets. The d -dimensional feature of one is produced by the ‘Emb’ layer, which is an extra fully-connected layer attached to FC-layer. The distances between image pairs are aggregated into a single loss value by a pre-defined loss function. The embedding space is optimized by iteratively minimizing this function loss.

This leads to a much faster convergence pace and better discriminativeness of the learned embedding space. The performance is further boosted by the mining of the hard negatives in [19, 15, 24, 2, 16].

In this paper, a simple but effective dynamic training sample mining strategy is proposed to boost the performance of deep metric learning. The idea is inspired by two observations, which largely diverge from the common beliefs in deep metric learning. On the one hand, it is commonly agreed that the images from the same category should be close to each other. However, we observe that it is harmful to the model if they are pushed as close as possible. The model could suffer from overfitting when the hard positives are pushed too close to each other. Hard negatives face the similar problem. On the other hand, it is true that the hard training samples are more informative than the easy ones. In order to attain a more discriminative model, these hard samples should be fed to the training with high priority. However, it will be more effective when they are fed to the training at the later stage, while leaving the process to learn from relatively easy examples at its early stage.

Based on the first observation, we only pull/push the positive/negative pairs above/below a similarity threshold to alleviate the over-fit issue. Based on the second observation, the impact of hard training samples is tuned dynamically, which is planted in the design of a loss function. Namely, unlike current practices in *N-Pair loss* [19], *lifted structure loss* [15], or *multiple similarity loss* [24], the hard training samples take higher effect as the training epoch grows. This mimics the cognitive process of human beings that learns general concepts from simple cases and drills deeper into the complex cases step by step. Considerable improvement is observed as this dynamic sampling strategy is integrated with *lifted structure loss*, *multiple similarity loss*, *triplet loss*, as well as *binomial deviance loss*. According to our experiments, such kind of improvement is consistent across different tasks such as fashion search, person re-identification, and fine-grained image search.

The remainder of this paper is organized as follows. Sec-

tion 2 reviews the most representative loss functions in deep metric learning. Our dynamic sampling strategy is presented in Section 3. The comparative study over the representative loss functions and the proposed sampling strategy is presented in Section 4. Section 5 concludes the paper.

2. Related Work

In this section, several representative loss functions and the enhancement strategies over them in deep metric learning are reviewed. In order to facilitate our later discussions, several concepts are defined. Given a pair of images $\{x_i, x_j\}$, the distance between them is given as

$$s_{i,j} = m(\mathcal{F}(x_i), \mathcal{F}(x_j)), \quad (1)$$

where $m(\cdot, \cdot)$ is a pre-defined distance measure. It could be *Cosine* similarity or *Euclidean* distance, etc. For clarity, the following discussion is made based on *Cosine* similarity by default. Correspondingly, the label for this image pair is given as $y_{i,j}$. Positive pair is given as $y_{i,j} = 1$, which indicates x_i and x_j come from the same category. While $y_{i,j}$ equals to 0 when they come from different categories. In the deep metric learning literature, the loss functions are mostly defined based on the positive and negative pairs, which are organized into a series of mini-batches for the sake of training efficiency.

Contrastive loss [5] encodes the similarities from both positive pairs and negative pairs in one loss function. Basically, it regularizes the similarities between positive pairs to be larger than the similarities from negative pairs with a constant margin λ . Namely,

$$\mathcal{L}_c = \frac{1}{m} \sum_{(i,j)}^{m/2} \left(-y_{i,j} s_{i,j} + (1 - y_{i,j}) [0, s_{i,j} - \lambda]_+ \right), \quad (2)$$

where m is the number of anchor-positive pairs in one training batch. $[\cdot]_+$ in Eqn. 2 is the hinge loss. In order to guarantee that there are sufficient anchor-positive pairs in one batch, a fixed number of positive pairs are selected for one

batch. The loss function neglects the fact that the dissimilar scales of two images to another image could be different. The minimization on \mathcal{L}_c tends to converge as long as the distance between one pair satisfies with the margin λ^1 . The loose constraint over the pairwise distance leads to slow convergence.

Binomial deviance loss (BD-loss) [26] can be viewed as a soft version of *contrastive loss*. Its loss function is given as

$$\mathcal{L}_b = \sum_{i=1}^m \left(\frac{1}{P} \sum_{y_{a,b}=1} \log [1 + e^{\alpha(\lambda - s_{a,b})}] + \frac{1}{N} \sum_{y_{c,d}=0} \log [1 + e^{\beta(s_{c,d} - \lambda)}] \right), \quad (3)$$

where P and N are the numbers of positive pairs and negative pairs respectively. α and β in Eqn. 3 are the scaling factors. Compared to hinge loss function in Eqn. 2, softplus function in Eqn. 3 demonstrates similar shape as hinge loss while is smooth and with continuous gradients. According to recent studies [26, 14], it shows superior performance in person re-identification, fashion search and fine-grained image search tasks.

In order to enhance the discriminativeness of the embedding space, *triplet loss* (defined in Eqn. 4) is designed to maximize the similarity between an anchor-positive pair $\{x_a, x_p\}$ in contrast to the similarity from anchor to a negative sample x_n .

$$\mathcal{L}_t = \frac{3}{2m} \sum_{i=1}^{m/2} [s_{a,n}^{(i)} - s_{a,p}^{(i)} + \lambda]_+ \quad (4)$$

Compared to *contrastive loss*, the gap between positive and negative pairs is defined in terms of relative similarity. Namely, the relative similarity between the positive and negative pair with respect to anchor. It therefore remains effective for various scenarios compared to that of *contrastive loss*. Nevertheless, it is expensive to enumerate all possible triplets in one mini-batch. As a result, some informative training samples may be left unused if no particular mining schemes are introduced.

In the literature, several efforts [18, 15, 2, 16] have been made to mine on the hard training samples to further boost its performance. In order to make full use of the samples inside one mini-batch, *lifted structure loss* (see Eqn. 5) [15] is proposed. The loss function is designed to consider all the positive and negative pairs in one mini-batch.

$$\mathcal{L}_f = \sum_{i=1}^m \left[\log \sum_{y_{i,j}=1} e^{\lambda - s_{i,j}} + \log \sum_{y_{i,j}=0} e^{s_{i,j}} \right]_+ \quad (5)$$

¹ λ acts as the minimum margin between positives and negatives for all the loss functions discussed in the paper.

The objective of *lifted structure loss* is to maximize the margin between negatives and positives. The negatives which are the closest to positive images are mined during the training. Because the optimization on nested maximum function converges to bad local optimum, the loss function is relaxed to optimize a smooth one.

Essentially, there are three types of negative pairs in the pair-based learning. Namely, they are the anchor-negative pairs, positive-negative pairs and negative-negative pairs. In the aforementioned models, they usually consider one or two of them while missing another. *Multiple similarity loss* [24] is proposed to consider the similarities from all three types of negative pairs. The loss function is given in Eqn. 6.

$$\mathcal{L}_m = \frac{1}{m} \sum_{i=1}^m \left(\frac{1}{\alpha} \log [1 + \sum_{k \in \mathcal{P}_i} e^{-\alpha(s_{i,k} - \lambda)}] + \frac{1}{\beta} \log [1 + \sum_{k \in \mathcal{N}_i} e^{\beta(s_{i,k} - \lambda)}] \right) \quad (6)$$

where α and β are the scaling parameters. In the above loss function, \mathcal{P}_i and \mathcal{N}_i are the positive and negative image sets respectively. Similar as *BD-loss*, the loss function is defined based on softplus function. In this learning model, the hard negatives are mined from the second type of pairs. The selected training samples are then weighted by the similarities from the other two types of pairs. According to [24], similar performance as *BD-loss* is reported.

In the literature, there are many efforts have been taken to enhance the performance of aforementioned models. For instance, online sampling is one of the typical ways. Conventionally, training samples are paired in advance, which might lead to over-fitting. In [19, 15, 24, 25], the training images are organized into pairs/triplets during the training so that one anchor can be paired with more number of samples.

Besides the loss function and sampling strategies, the batch size and scaling parameters in the loss function (*e.g.*, α in Eqn. 3) are the other two factors impact the performance. Larger batch size allows the loss function to consider more pairwise/triangular relationships among images. This in turn leads to a better embedding space structure. However, large batch size also leads to higher computation complexity. As a result, a trade-off has to be made. The scaling factors are the few hyper-parameters have to be tuned manually in many loss functions such as *BD-loss* and *multiple similarity loss*. According to recent study [24], the parameter tuning alone could lead to 20% performance improvement.

In our solution, the training samples selection is novelly abstracted to weighting terms and integrated with the loss function. It allows the training process to learn the embedding space in an order, namely from relatively easy samples

to the harder. Therefore, the hard concepts (carried by hard samples) are learned without overwriting the learned general (easy) concept. Moreover, this scheme is generic in the sense it could be integrated with various loss functions. Its effectiveness is confirmed on fashion search, person re-identification, and fine-grained image search when it is integrated with *lifted structure loss*, *multiple similarity loss*, *triplet loss*, and *BD-loss*.

3. Dynamic Training Pair Selection

In this section, our strategies that are designed to boost the performance of deep metric learning are presented. In general, most of the deep metric learning approaches are defined based on training image pairs. The variations across different approaches mainly lie in the selection of training pairs and the definition of loss function. In this section, we first present the heuristics we used in the training pair selection. Based on the heuristics, various existing loss functions, that are integrated with two dynamic sampling terms, are presented.

3.1. Heuristics in Pairs Mining

As witnessed in many research works [15, 24, 2, 16], the easy training samples take a large portion in a mini-batch, however they are less helpful than the hard training pairs. Similar as other works [25], hard thresholds are set to filter out these easy training samples. To achieve that, two similarity thresholds τ_p and τ_n , namely one for easy positives and another for easy negative pairs, are introduced. Given the similarity between a positive pair $\{x_i, x_j\}$ is $s_{i,j}$, positive pair $\{x_i, x_j\}$ will not be considered in the training if $s_{i,j} \geq \tau_p$. Similarly, a negative pair $\{x_k, x_m\}$ is not considered in the training as $s_{k,m} \leq \tau_n$. In our implementation, τ_p and τ_n are set to 0.9 and 0.1 respectively. As the training continues, the boundary between positives and negatives becomes clearer. One could imagine more and more negative and positive pairs will be filtered out by these two thresholds and therefore will no longer join in the training.

In addition to τ_p and τ_n , similar as [24], a flexible margin is set for negative pairs to separate them from the most remote positive pairs. Namely, given a positive pair $\{x_i, x_k\}$ and a negative pair $\{x_i, x_j\}$, $\{x_i, x_j\}$ will be selected to join in the training when the following inequation holds.

$$s_{i,j} > \min_{y_{i,k}=1} s_{i,k} - \tau_b, \quad (7)$$

where τ_b is the lower bound similarity of a positive sample to the anchor.

The roles that these three thresholds take are illustrated in Fig. 2. On the one hand, threshold τ_p prevents the training from pushing the positives as close as possible. On the other hand, threshold τ_n prevents the negative pairs from being pulled too far away. These two thresholds together prevent

the structure of the learned embedding space from collapsing due to overfitting. According to our observation, very few training samples could pass through these two thresholds at the early training stage. As the training continues for several rounds, more and more negative pairs and positives are well separated in the embedding space. They are, therefore, set aside by these two thresholds. The training gets focus more and more on harder training samples. The flexible threshold given by Inequation 7 takes similar effect. As one could imagine, $\min_{y_{i,k}=1} s_{i,k}$ is relatively small at the early training stage. As the embedding space evolves to a better structure, $\min_{y_{i,k}=1} s_{i,k}$ grows bigger. This in turn thresholds out more and more relatively easy training samples.

3.2. Dynamic Metric Learning Loss

Based on the above heuristics, only relatively hard pairs are joined in the training. Among these relatively hard training samples, the degree of hardness still varies from one training pair to another. In the ideal scenario, it is expected that the training samples are organized sequentially according to the degree of hardness. Samples with low degree of hardness are fed to the training at the early stages. As the training model evolves, harder training samples are fed to the training process since they become more critical to define the category borders. Intuitively, one has to prepare a group of image pairs for training with increasing degree of hardness each time. Although it sounds plausible, it is hard to operate as the hardness degree of one image pair varies along with the evolving embedding space. In the following, a novel weighting strategy based on image pair similarity $s_{i,j}$ is proposed. It regularizes the importance of a training pair according to its hardness in the training. The easy training samples are assigned with higher importance at the early training stages and the importance of hard ones grows as the training epoch increases.

In the existing loss functions, the similarity between one pair of image $s_{a,b}$ is mainly designed to weight how much penalty we should be aggregated into the loss function. In our design, it is additionally used to indicate the degree of a pair joined in one round of training. Specifically, for a positive pair $\{a, b\}$, the value $\tau_p - s_{a,b}$ basically indicates the hardness degree. The larger this value is, the harder the positive pair is. The value $s_{c,d} - \tau_n$ has the similar efficacy for a negative pair $\{c, d\}$. Let's take *BD-loss* as an example. We show how the training samples are re-weighted according to their degree of hardness. Given E_t is the number of total epochs we need to train our model, the current number of epochs that the training has been undertaken is given as E_c ($1 \leq E_c \leq E_t$). Two terms $\frac{2E_c}{E_t}(\tau_p - s_{a,b})^2$ and $\frac{2E_c}{E_t}(s_{c,d} - \tau_n)^2$, one for positive and one for negative, are introduced to *BD-loss*. The loss function in Eqn. 3 is rewrit-

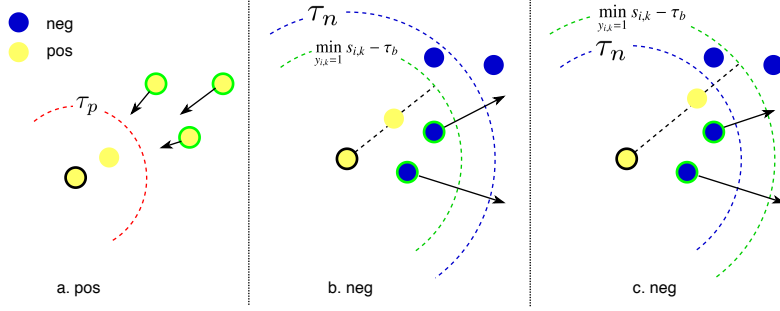


Figure 2. The illustration of the role of three thresholds. The dashed circles in red, blue, and green represent borders regularized by τ_p , τ_n and Inequation 7 respectively. In figure (a), the positive samples which meet with $s_{i,k} < \tau_p$ will be selected. For negative pairs, they could be in either cases illustrated in figure (b) or figure (c). Under figure (b) and (c) cases, the negative pair $\{i, j\}$ that $s_{i,j} > \tau_n$ and $s_{i,j} > \min_{j_k=1} s_{i,k} - \tau_b$ will be selected.

ten as

$$\mathcal{L}_b^* = \sum_{i=1}^m \left\{ \frac{1}{P} \sum_{y_{a,b}=1} \log \left[1 + e^{\alpha[(\lambda - s_{a,b}) + \frac{2E_c}{E_t}(\tau_p - s_{a,b})^2]} \right] + \frac{1}{N} \sum_{y_{c,d}=0} \log \left[1 + e^{\beta[(s_{c,d} - \lambda) + \frac{2E_c}{E_t}(s_{c,d} - \tau_n)^2]} \right] \right\}. \quad (8)$$

Apparently, these two terms are impacted by both E_c and the image pair similarity s . On the one hand, the larger the gap between s and the corresponding bound (either τ_p or τ_n) is, the higher these two terms are. This basically indicates the degree of hardness for a training pair (either positive or negative). Hard pairs tend to hold high weights. On the other hand, the terms are also controlled by the number of current epochs. The more number of epochs the training is undertaken, the higher of impact these two terms have on the overall loss \mathcal{L}_b^* . This leads the optimization to focusing on these hard training pairs more and more as E_c grows bigger.

Similarly, for *lifted structure loss* (Eqn. 5), *triplet loss* (Eqn. 4) and *multiple similarity loss* (Eqn. 6), they are rewritten as Eqn. 9, Eqn. 10 and Eqn. 11 if these two terms are integrated.

$$\mathcal{L}_f^* = \sum_{i=1}^m \left\{ \log \sum_{y_{a,b}=1} e^{[(\lambda - s_{a,b}) + \frac{2E_c}{E_t}(\tau_p - s_{a,b})^2]} + \log \sum_{y_{c,d}=0} e^{[s_{c,d} + \frac{2E_c}{E_t}(s_{c,d} - \tau_n)^2]} \right\} + \quad (9)$$

$$\mathcal{L}_t^* = \frac{3}{2m} \sum_{i=1}^{m/2} \left\{ \frac{1}{P} \sum_{y_{a,b}=1} \left[-s_{a,b} + \frac{2E_c}{E_t}(\tau_p - s_{a,b})^2 \right] + \frac{1}{N} \sum_{y_{c,d}=0} \left[s_{c,d} + \frac{2E_c}{E_t}(s_{c,d} - \tau_n)^2 \right] + \lambda \right\} + \quad (10)$$

$$\mathcal{L}_m^* = \frac{1}{m} \sum_{i=1}^m \left\{ \frac{1}{\alpha} \log \left[1 + \sum_{a \in \mathcal{P}_i} e^{[-\alpha(s_{i,a} - \lambda) + \frac{2E_c}{E_t}(\tau_p - s_{i,a})^2]} \right] + \frac{1}{\beta} \log \left[1 + \sum_{b \in \mathcal{N}_i} e^{[\beta(s_{i,b} - \lambda) + \frac{2E_c}{E_t}(s_{i,b} - \tau_n)^2]} \right] \right\} \quad (11)$$

In Eqn. 9, Eqn. 10, and Eqn. 11, terms $\frac{2E_c}{E_t}(\tau_p - s_{a,b})^2$ and $\frac{2E_c}{E_t}(s_{c,d} - \tau_n)^2$ play a similar role as they do on *BD-loss*. Fig. 3 shows the weights produced by term $\frac{2E_c}{E_t}(\tau_p - s_{a,b})^2$ for positive pair with respect to $s_{a,b}$. The similarity of a positive pair $s_{a,b}$ is in the range of $[0.0, 0.9]$ after thresholding by τ_p . Low $s_{a,b}$ indicates the positive pair is close to the category boundary, namely it is a hard positive pair. As shown in the figure, the weights we assign to all the pairs are equally low at the first epoch of the training. The impact of this term on the loss function is therefore minor. Since the easy pairs take a large portion in one mini-batch, the training is actually biased towards easy pairs at the early stages. As epoch E_c grows, higher weights are assigned to pairs with lower similarities (as shown by the green curve in Fig. 3). The bias towards hard positives is more significant as epoch E_c grows even bigger, which in turn leads to the higher contribution from hard positives to the loss function. Similar thing happens to the term for negative pairs. As a consequence, the optimization on the above models is tuned to focusing on the hard pairs gradually as the epoch grows.

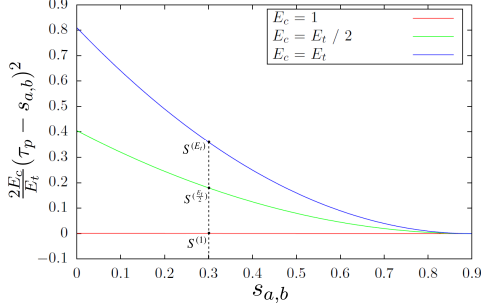


Figure 3. The illustration of re-weighting term for positive pairs. The term is given as the function of similarity $s_{a,b}$. This term assigns different weights to different positive pairs according to their mutual similarities. The weights vary as the epoch E_c grows. The figure shows the re-weighting curves when training is at 1st, $E_t/2$ -th and E_t -th epoch. As E_c grows, re-weighting is biased towards hard training pairs (whose $s_{a,b}$ is low). This leads to the higher contribution to the final loss.

As will be revealed in the experiment section, the simple modification on these popular loss functions leads to considerable performance enhancement. The performance wins over the original model could be as high as more than 100%.

The advantages of such modification are three folds. Firstly, the training samples are fed to the model from easy to hard as the training epoch grows. This allows the training process to focus on relatively easy samples at the early stage and hard samples at its later stage. Secondly, this training sample selection rule is integrated with the loss function, no extra complexity is induced. Moreover, it is a generic strategy as it is compatible with different types of loss functions.

3.3. Implementation Details

The pre-trained Inception [9] is employed as the backbone network for our deep metric learning. Each training image is first fed into the network to generate a fixed-length feature vector, which maps the image into the embedding space. The size of the feature vector is typically set to 512 in our study. Thereafter, the images are organized into mini-batches. In each training epoch, 25 classes are randomly selected. Five images are randomly selected from each of these classes. This results in 125 images in one mini-batch. Thereafter, the pairwise similarity within this mini-batch is calculated. The image pairs which pass through the thresholds τ_p, τ_n and satisfy with Inequation 7 are selected to join in the training. To this end, the loss is computed based on the revised loss function. For instance, Eqn. 8 is employed for *BD-loss*. The computed loss for one mini-batch is back-propagated to optimize the network. $\alpha, \lambda,$ and β in Eqn. 8 are set to 2, 0.5, and 40 respectively. The above training process loops for E_t rounds.

For *lifted structure loss, triplet loss, and multiple similar-*

ity loss, the training process remains largely the same. The only difference lies in the loss function. For *lifted structure loss, triplet loss, and multiple similarity loss*, Eqn. 9, Eqn. 10 and Eqn. 11 are employed respectively. λ in Eqn. 9 is set to 1.0. λ in Eqn. 10 is set to 0.5. $\alpha, \lambda,$ and β in Eqn. 11 are set to 2, 0.5, and 50 respectively. All the codes are implemented with PyTorch and are available on GitHub².

4. Experiments

In this section, the effectiveness of the proposed dynamic hard training sample mining strategy is studied when it is integrated with four popular loss functions. Namely, they are *BD-loss* (BD), *triplet loss* (TP), *multiple similarity loss* (MS), and *lifted structure loss* (LF). They are denoted as BD*, TP*, MS*, and LF* respectively when the proposed dynamic sampling strategy is integrated. The study is made on three different tasks, namely fashion search, fine-grained image search, and person re-identification. The behavior of these popular loss functions on these three tasks are comprehensively studied. The performance from each loss function is also compared to state-of-the-art approaches in each particular task.

4.1. Datasets and Evaluation Protocols

For fashion search, datasets In-Shop (also known as Deepfashion) [13] and Deepfashion2 [3] are adopted in the evaluation. Dataset *In-Shop* is a collection of fashion product images crawled from online shopping websites. There are 52,712 images covering across 7,982 classes. 14,218 images are set aside as the queries. For dataset *Deepfashion2*, it is comprised of images both from online shops and users. Considerable portion of the images are directly collected from *Deepfashion*. For *Deepfashion2*, the retrieval is defined as user-to-shop query. Namely, the images uploaded by the users are treated as queries. The same product images crawled from online shopping websites are treated as search targets. It is more challenging than *In-Shop* task as it is a cross-domain search problem. Since the test set for *Deepfashion2* is not released yet, the validation set is treated as the candidate dataset for search evaluation.

For fine-grained image search, *CUB-200-2011* [22] and *CARS196* [12] are adopted, both of which are the most popular evaluation benchmarks in deep metric learning. *CUB-200-2011* covers 200 bird categories. Following the conventional practice, 5,864 images of 100 categories are used for training, and the remaining 5,924 images from 100 categories are used for evaluation. Dataset *CARS196*, is comprised of 16,185 car images that cover across 196 categories. The 8,054 images from 98 classes are used for training. The rest 8,131 images from the same group of classes are used for testing.

²<https://github.com/CH-Liang/DSDML>

Table 1. Summary over five datasets used in the evaluation

Datasets	#Images	#Train	#Query	#Test/Validation	Task
In-shop [13]	52,712	25,882	14,218	12,612	Fashion search
Deepfashion2 [3]	224,389	191,961	10,990	21,438	Fashion search
CUB200 [22]	11,788	5,864	-	5,924	fine-grained search
Cars-196 [12]	16,185	8,054	-	8,131	fine-grained search
Market-1501 [27]	36,036	12,936	3,368	19,732	Re-Identification

Table 2. Ablation analysis of BD-loss on Deepfashion2 validation set

Recall@	Dim.	1	5	10	20
BD	512	40.2	55.4	62.7	70.1
BD+T	512	41.6	57.0	63.7	70.5
BD+W	512	42.9	58.5	65.7	72.8
<i>BD*</i>	512	44.0	60.2	67.2	73.7

On person re-identification task, the experiments are conducted on *Market-1501* [27] dataset. It consists of 32,668 images from 1,501 individuals. They are captured by 6 cameras of different viewpoints. In the training, 12,936 images from 750 individuals are used. This setting is fixed for all the evaluation approaches. The brief information about all the five datasets are summarized in Tab. 1.

In our implementation, images from all datasets are resized to 256×256 and then randomly cropped to 224×224 . For data augmentation, we followed the configurations in [15]. Specifically, random cropping and random horizontal flips are employed during training and single cropping is employed during testing. The backbone network for all the four loss functions we considered is Inception [9]. The Adam optimizer is adopted in the training. Following the convention in the literature, we report our performance in terms of Recall@K. To be line with the evaluation convention on different benchmarks, difference series of Ks are taken on different datasets. All the experiments are pulled out on a server with NVIDIA GTX 1080 Ti GPU setup.

4.2. Ablation Study with Fashion Search

Before we show the performance improvement that the overall dynamic sampling strategy brings for different loss functions, the study on the contribution of each step in dynamic sampling to the final improvement is presented. The study is typically conducted with *BD-loss* on the fashion search task. However, the similar trend is observed on other loss functions and other tasks. In the experiment, the *BD-loss* that is integrated with simple thresholding with τ_p , τ_n and Inequation 7 is given as “BD+T”. While *BD-loss* integrated with two re-weighting terms only is given as “BD+W”. *BD-loss* integrated with both is given as *BD**. The results of these three runs on *Deepfashion2* are shown in Tab. 2. The result from *BD-loss* is treated as the comparison baseline.

As shown in the table, both schemes achieve consistent improvement. On average, the dynamic sampling brings more considerable improvement than simple thresholding. Specifically, more than 2% improvement is observed on “BD+W” run across different Ks. The best performance is observed when two schemes are integrated as a whole. This basically indicates they are complementary to each other. In the following experiments, all the four loss functions we study here are integrated with these two enhancement schemes.

4.3. Fashion Search

In this section, the effectiveness of the proposed enhancement strategy on four loss functions is studied in fashion search task. Representative approaches in the literature on this task are considered in the study. FashionNet [13] and Match R-CNN [3] are treated as the comparison baselines for *In-Shop* and *Deepfashion2* respectively. They are proposed along with these two benchmarks. The fashion search is treated as a sub-task under the multi-task learning framework. In addition, recent deep metric learning approaches Divide and Conquer (Divide) [17], Mining Interclass Characteristics (MIC) [16], *Angular loss* (Angular) [23], *Batch hard triplet loss* (Hard Triplet) [6] and *N-Pair loss* (N-Pair) [19] are also considered in the comparison. Among these approaches, MIC learns auxiliary encoder for the visual attributes, which induces extra computational costs. Attention-based Ensemble (ABE) [11] is the representative approach of ensemble deep metric learning.

The performance on *In-Shop* and *Deepfashion2* is shown on Tab. 3 and Tab. 4 respectively. As shown in Tab. 3 and Tab. 4, all the four loss functions which are integrated with dynamic sampling terms demonstrate considerable performance improvement. The improvement ranges from 10-100% for different loss functions. Enhanced by the dynamic sampling, the performance from all loss functions become competitive to or even outperforms the most effective approach in the literature, in particular on the challenging dataset *Deepfashion2*. An interesting observation is that the performance difference between different loss functions becomes much smaller when being all supported by the dynamic sampling. Overall, *BD-loss* with dynamic sampling shows the best performance on the two datasets. The performance from *BD** is similar as the one reported in [14], which however requires product attributes in the training.

Table 3. Comparison with the state-of-the-art approaches on *In-Shop*

Recall@	Dim.	1	10	20	30	40	50
FashionNet [‡] [13]	4,096	53.0	73.0	76.0	77.0	79.0	80.0
Divide [‡] [17]	128	85.7	95.5	96.9	97.5	-	98.0
ABE [‡] [11]	512	87.3	96.7	97.9	98.2	98.5	98.7
MIC [‡] [16]	128	88.2	97.0	-	98.0	-	98.8
BD	512	87.3	96.1	97.4	97.9	98.2	98.4
BD*	512	89.8	97.6	98.3	98.6	98.8	98.9
LF	512	35.3	65.5	73.6	77.9	80.6	82.5
LF*	512	81.5	93.8	95.7	96.5	97.1	97.4
MS	512	87.3	96.3	97.3	98.0	98.3	98.5
MS*	512	87.7	96.7	97.6	98.1	98.4	98.7
TP	512	83.7	94.5	96.2	97.0	97.4	97.7
TP*	512	84.7	95.1	96.6	97.2	97.6	97.9

[‡] digits are cited from the referred paper.

Table 4. Comparison with the state-of-the-art approaches on *Deep-fashion2* validation set

Recall@	Dim.	1	5	10	20
Match R-CNN [‡] [3]	256	26.8	-	57.4	66.5
Angular [‡] [23]	128	32.4	47.9	55.3	62.3
Hard Triplet [‡] [6]	128	32.4	48.9	56.0	63.2
N-Pair [‡] [19]	128	32.8	50.1	57.9	64.8
MIC [16]	512	38.1	52.1	59.3	66.3
Divide [17]	512	39.4	54.4	61.5	68.5
BD	512	40.2	55.4	62.7	70.1
BD*	512	44.0	60.2	67.2	73.7
LF	512	15.7	28.3	35.3	43.3
LF*	512	39.3	55.5	63.3	70.6
MS	512	41.0	55.9	62.7	70.2
MS*	512	42.4	58.0	65.2	72.5
TP	512	38.6	54.1	61.6	68.9
TP*	512	41.2	57.0	64.4	71.9

[‡] digits are cited from the referred paper.

The search result samples from BD* on *DeepFashion2* are shown in Fig. 4. As shown in the figure, there are some false positives, nevertheless they are reasonable in the sense that they look very similar to the queries. Moreover, our approach shows steady performance even under severe variations in illumination and image quality.

4.4. Fine-grained search

In this section, the performance of the enhanced loss functions is evaluated on *CUB-200-2011* and *CARS196* for fine-grained search. Three state-of-the-art deep metric learning approaches Divide [17], ABE [11] and MIC [16] are considered in the comparison. The performance results on these two datasets are shown in Tab. 5 and Tab. 6. respectively.

The performance from all enhanced loss functions show consistent improvement over the original ones. The improvement is particularly significant on *lifted structure loss*. BD* and MS* perform competitively well with the state-

of-the-art approaches, namely Divide and MIC. Compared to Divide and MIC, our approach is much lightweight. Approach Divide requires to learn several sub-embedding spaces. Similarly, extra computation is required in MIC to train the auxiliary encoder for the latent visual attributes. In contrast, considerable improvement from our approach is achieved by injecting two re-weighting terms into the loss function. No sophisticated modification on the training process or the network architecture is required.

Table 5. Comparison with the state-of-the-art approaches on *CUB200*

Recall@	Dim.	1	2	4	8	16	32
ABE [‡] [11]	512	60.6	71.5	79.8	87.4	-	-
Divide [‡] [17]	128	65.9	76.6	84.4	90.6	-	-
MIC [‡] [16]	128	66.1	76.8	85.6	-	-	-
BD	512	63.5	74.5	82.8	88.9	93.6	96.6
BD*	512	63.8	75.1	83.3	89.7	94.1	96.8
LF	512	47.2	59.1	70.3	80.3	87.2	92.4
LF*	512	54.9	66.7	77.3	84.8	90.6	94.6
MS	512	64.3	75.0	83.3	89.6	93.9	96.8
MS*	512	64.8	75.1	84.0	90.3	94.1	96.9
TP	512	52.4	63.9	73.7	82.4	89.4	93.6
TP*	512	55.2	66.3	76.5	84.5	90.5	94.4

[‡] digits are cited from the referred paper.

Table 6. Comparison with the state-of-the-art approaches on *Cars-196*

Recall@	Dim.	1	2	4	8	16	32
ABE [‡] [11]	512	85.2	90.5	94.0	96.1	-	-
Divide [‡] [17]	128	84.6	90.7	94.1	96.5	-	-
MIC [‡] [16]	128	82.6	89.1	93.2	-	-	-
BD	512	79.7	86.9	91.9	95.1	97.1	98.4
BD*	512	81.2	88.3	92.8	95.8	97.6	98.8
LF	512	37.9	49.8	61.4	72.0	81.7	88.6
LF*	512	63.6	73.5	81.4	87.8	92.4	95.5
MS	512	81.1	88.0	92.6	95.4	97.4	98.6
MS*	512	81.6	88.3	92.9	95.8	97.6	98.8
TP	512	55.4	66.5	75.6	83.4	89.1	93.4
TP*	512	63.2	73.5	81.6	87.7	92.4	95.4

[‡] digits are cited from the referred paper.

4.5. Person Re-Identification

In this section, we further study the effectiveness of the proposed strategy on person re-identification task. The experiment is conducted on *Market-1501*. State-of-the-art approaches BoW+CN [27], Pose-driven Deep Convolutional (PDC) [20] and Part-based Convolutional Baseline (PCB) [21] are considered in the comparison. BoW+CN is proposed along with dataset *Market-1501*. It is the color names descriptor (CN) quantized with bag-of-words (BoW). BoW+CN is treated as comparison baseline in this study. Both PDC and PCB build feature representations on body-parts level. Namely, sub-feature vector is learned on each

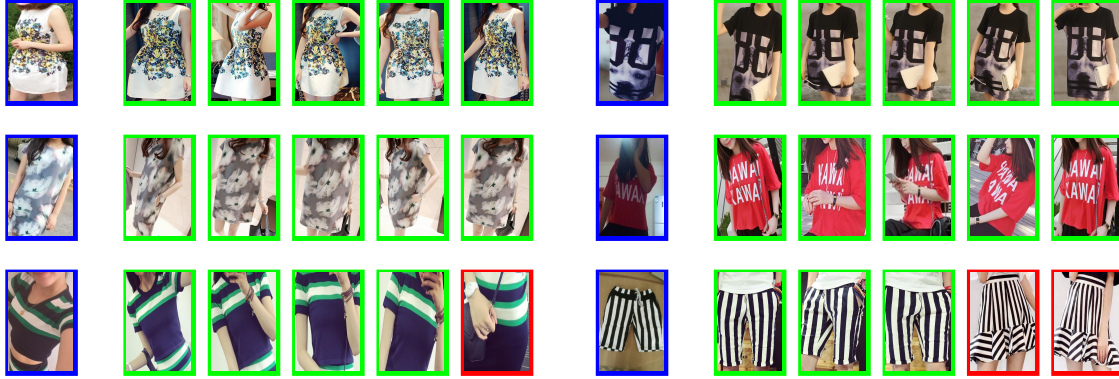


Figure 4. Top-5 search results on *Deepfashion2*. The queries are shown on the first column and followed by retrieved top-5 candidates on each row.

body part (e.g., head and legs), which requires fine-grained annotations as well. The performance from all the approaches is shown in Tab. 7.

On the one hand, it is clear to see the consistent improvement of the proposed strategy brings to various loss functions. In particular, the improvement is significant for *lifted structure loss*. All the approaches with the enhanced loss functions outperform the comparison baseline. On the other hand, there is a large performance gap between these deep metric learning based models and the state-of-the-art approaches of person re-identification. This is not surprising given more complex model and more training information are involved for these two state-of-the-art approaches. In contrast, only category information is capitalized in deep metric learning approaches. Nevertheless, this experiment does confirm that the improvement achieved by dynamic sampling is consistent across various visual retrieval tasks. It also shows how well deep metric learning approach alone could achieve on this complicated task.

Table 7. Comparison with the state-of-the-art approaches on Market-1501 for person re-identification task

Recall@	Dim.	1	5	10	20
BoW+CN [‡] [27]	100	47.3	-	-	-
PDC [‡] [20]	2,048	84.1	92.7	94.9	96.8
PCB [‡] [21]	12,288	93.8	97.5	98.5	-
BD	512	60.9	82.6	88.2	92.1
BD*	512	61.0	83.3	89.4	92.3
LF	512	31.0	53.2	62.3	71.3
LF*	512	52.0	74.5	81.7	87.8
MS	512	62.0	83.7	89.3	92.6
MS*	512	63.0	84.4	89.6	93.2
TP	512	49.4	73.0	79.8	86.3
TP*	512	53.5	76.4	83.1	87.8

[‡] digits are cited from the referred paper.

Overall, *BD-loss* and *multiple similarity loss* show much more superior performance over other loss functions on three different tasks. With the proposed dynamic sampling

strategy, both models demonstrate performance boosts on three different tasks and across different parameter settings. In particular, the performance from the enhanced *BD-loss* and *multiple similarity loss* is better than or close to state-of-the-art approaches on fashion search and fine-grained search tasks.

5. Conclusion

We have presented a simple but effective dynamic sampling strategy to boost the performance of deep metric learning. In our solution, the dynamic sampling is formulated as two terms that are compatible with various loss functions. These two re-weighting terms dynamically tune the impact that a training pair contribute to the loss function. Higher weights are assigned to the easy training pairs at the early training stages. Hard pairs are assigned with increasingly higher weights as the training epoch grows. This allows the network to learn the concepts from easy to hard, which is comparable to the cognitive process of human beings. Experiments on five datasets of three different tasks show consistent performance improvement when this strategy is integrated with four popular loss functions. In addition, we find that *BD-loss* and *multiple similarity loss* are consistently better on three different tasks than the other loss functions by large performance margins.

References

- [1] Sumit Chopra, Raia Hadsell, and Yann LeCun. Learning a similarity metric discriminatively, with application to face verification. In *2005 IEEE Computer Society Conference on Computer Vision and Pattern Recognition (CVPR'05)*, volume 1, pages 539–546. IEEE, 2005.
- [2] Weifeng Ge. Deep metric learning with hierarchical triplet loss. In *Proceedings of the European Con-*

- ference on Computer Vision (ECCV), pages 269–285, 2018.
- [3] Yuying Ge, Ruimao Zhang, Xiaogang Wang, Xiaoou Tang, and Ping Luo. Deepfashion2: A versatile benchmark for detection, pose estimation, segmentation and re-identification of clothing images. In *Proceedings of the IEEE Conference on Computer Vision and Pattern Recognition*, pages 5337–5345, 2019.
- [4] M Hadi Kiapour, Xufeng Han, Svetlana Lazebnik, Alexander C Berg, and Tamara L Berg. Where to buy it: Matching street clothing photos in online shops. In *Proceedings of the IEEE international conference on computer vision*, pages 3343–3351, 2015.
- [5] Raia Hadsell, Sumit Chopra, and Yann LeCun. Dimensionality reduction by learning an invariant mapping. In *2006 IEEE Computer Society Conference on Computer Vision and Pattern Recognition (CVPR'06)*, volume 2, pages 1735–1742. IEEE, 2006.
- [6] Alexander Hermans, Lucas Beyer, and Bastian Leibe. In defense of the triplet loss for person re-identification. *arXiv preprint arXiv:1703.07737*, 2017.
- [7] Elad Hoffer and Nir Ailon. Deep metric learning using triplet network. In *International Workshop on Similarity-Based Pattern Recognition*, pages 84–92. Springer, 2015.
- [8] Junshi Huang, Rogerio S Feris, Qiang Chen, and Shuicheng Yan. Cross-domain image retrieval with a dual attribute-aware ranking network. In *Proceedings of the IEEE international conference on computer vision*, pages 1062–1070, 2015.
- [9] Sergey Ioffe and Christian Szegedy. Batch normalization: Accelerating deep network training by reducing internal covariate shift. *arXiv preprint arXiv:1502.03167*, 2015.
- [10] Xin Ji, Wei Wang, Meihui Zhang, and Yang Yang. Cross-domain image retrieval with attention modeling. In *Proceedings of the 25th ACM international conference on Multimedia*, pages 1654–1662, 2017.
- [11] Wonsik Kim, Bhavya Goyal, Kunal Chawla, Jungmin Lee, and Keunjoo Kwon. Attention-based ensemble for deep metric learning. In *Proceedings of the European Conference on Computer Vision (ECCV)*, pages 736–751, 2018.
- [12] Jonathan Krause, Michael Stark, Jia Deng, and Li Fei-Fei. 3d object representations for fine-grained categorization. In *Proceedings of the IEEE international conference on computer vision workshops*, pages 554–561, 2013.
- [13] Ziwei Liu, Ping Luo, Shi Qiu, Xiaogang Wang, and Xiaoou Tang. Deepfashion: Powering robust clothes recognition and retrieval with rich annotations. In *Proceedings of the IEEE conference on computer vision and pattern recognition*, pages 1096–1104, 2016.
- [14] Dipu Manandhar, Muhammet Bastan, and Kim-Hui Yap. Semantic granularity metric learning for visual search. *arXiv preprint arXiv:1911.06047*, 2019.
- [15] Hyun Oh Song, Yu Xiang, Stefanie Jegelka, and Silvio Savarese. Deep metric learning via lifted structured feature embedding. In *Proceedings of the IEEE conference on computer vision and pattern recognition*, pages 4004–4012, 2016.
- [16] Karsten Roth, Biagio Brattoli, and Bjorn Ommer. Mic: Mining interclass characteristics for improved metric learning. In *Proceedings of the IEEE International Conference on Computer Vision*, pages 8000–8009, 2019.
- [17] Artsiom Sanakoyeu, Vadim Tschernezki, Uta Buchler, and Bjorn Ommer. Divide and conquer the embedding space for metric learning. In *Proceedings of the IEEE Conference on Computer Vision and Pattern Recognition*, pages 471–480, 2019.
- [18] Florian Schroff, Dmitry Kalenichenko, and James Philbin. Facenet: A unified embedding for face recognition and clustering. In *Proceedings of the IEEE conference on computer vision and pattern recognition*, pages 815–823, 2015.
- [19] Kihyuk Sohn. Improved deep metric learning with multi-class n-pair loss objective. In *Advances in neural information processing systems*, pages 1857–1865, 2016.
- [20] Chi Su, Jianing Li, Shiliang Zhang, Junliang Xing, Wen Gao, and Qi Tian. Pose-driven deep convolutional model for person re-identification. In *Proceedings of the IEEE international conference on computer vision*, pages 3960–3969, 2017.
- [21] Yifan Sun, Liang Zheng, Yi Yang, Qi Tian, and Shengjin Wang. Beyond part models: Person retrieval with refined part pooling (and a strong convolutional baseline). In *Proceedings of the European Conference on Computer Vision (ECCV)*, pages 480–496, 2018.
- [22] Catherine Wah, Steve Branson, Peter Welinder, Pietro Perona, and Serge Belongie. The caltech-ucsd birds-200-2011 dataset. 2011.
- [23] Jian Wang, Feng Zhou, Shilei Wen, Xiao Liu, and Yuanqing Lin. Deep metric learning with angular loss. In *Proceedings of the IEEE International Conference on Computer Vision*, pages 2593–2601, 2017.
- [24] Xun Wang, Xintong Han, Weilin Huang, Dengke Dong, and Matthew R Scott. Multi-similarity loss with general pair weighting for deep metric learning. In *Proceedings of the IEEE Conference on Com-*

puter Vision and Pattern Recognition, pages 5022–5030, 2019.

- [25] Xinshao Wang, Yang Hua, Elyor Kodirov, Guosheng Hu, Romain Garnier, and Neil M Robertson. Ranked list loss for deep metric learning. In *Proceedings of the IEEE Conference on Computer Vision and Pattern Recognition*, pages 5207–5216, 2019.
- [26] Dong Yi, Zhen Lei, and Stan Z Li. Deep metric learning for practical person re-identification. *arXiv preprint arXiv:1407.4979*, 2014.
- [27] Liang Zheng, Liyue Shen, Lu Tian, Shengjin Wang, Jingdong Wang, and Qi Tian. Scalable person re-identification: A benchmark. In *Computer Vision, IEEE International Conference on*, 2015.